A Letters Journal Exploring the Frontiers of Physics

OFFPRINT

Time-series based prediction of complex oscillator networks via compressive sensing

W.-X. Wang, R. Yang, Y.-C. Lai, V. Kovanis and M. A. F. Harrison

EPL, **94** (2011) 48006

epl A Letters Journal Exploring the Frontiers of Physics

May 2011

EPL, **94** (2011) 48006
doi: 10.1209/0295-5075/94/48006

www.epljournal.org

Time-series–based prediction of complex oscillator networks via compressive sensing

Wen-Xu Wang[1(a)], Rui Yang[1], Ying-Cheng Lai[1,2], Vassilios Kovanis[3] and Mary Ann F. Harrison[4]

[1] *School of Electrical, Computer and Energy Engineering, Arizona State University - Tempe, AZ 85287, USA*
[2] *Department of Physics, Arizona State University - Tempe, AZ 85287, USA*
[3] *Sensors Directorate - 2241 Avionics Circle,Wright Patterson AFB, OH 45433, USA*
[4] *Physical Sciences and Technology, Scientific Research Group, WVHTC Foundation - Fairmont, WV 26554, USA*

received 17 December 2010; accepted in final form 13 April 2011
published online 16 May 2011

PACS 89.75.Hc – Networks and genealogical trees
PACS 89.20.Hh – World Wide Web, Internet
PACS 05.10.-a – Computational methods in statistical physics and nonlinear dynamics

Abstract – Complex dynamical networks consisting of a large number of interacting units are ubiquitous in nature and society. There are situations where the interactions in a network of interest are unknown and one wishes to reconstruct the full topology of the network through measured time series. We present a general method based on compressive sensing. In particular, by using power series expansions to arbitrary order, we demonstrate that the network-reconstruction problem can be casted into the form $\mathbf{X} = \mathbf{G} \cdot \mathbf{a}$, where the vector $\mathbf{X}$ and matrix $\mathbf{G}$ are determined by the time series and $\mathbf{a}$ is a sparse vector to be estimated that contains all nonzero power series coefficients in the mathematical functions of all existing couplings among the nodes. Since $\mathbf{a}$ is sparse, it can be solved by the standard L_1-norm technique in compressive sensing. The main advantages of our approach include sparse data requirement and broad applicability to a variety of complex networked dynamical systems, and these are illustrated by concrete examples of model and real-world complex networks.

In network science, previous efforts have been mostly on network structures and their effects on various dynamical processes taking place on or supported by the network. The types of processes that have been under intense investigations include synchronization, virus spreading, traffic flow, and cascading failures [1]. A typical approach in the field is to implement a particular dynamical process of interest on networks whose connecting topologies are completely specified. While this line of research is necessary for discovering and understanding various fundamental phenomena in complex networks, the importance of devising a general solution to the inverse problem of network prediction has been increasingly recognized [2–5]. For example, in biological sciences, a significant task is to reconstruct a variety of networks from experimental data such as inferring gene regulation networks from gene expression data [6–9]. Another example is the application of spike classification methods [10–12] to detecting interactions among neurons. Quite recently, it was demonstrated that the hierarchical property in many complex networks can be used to predict missing links [13]. Despite the success of the various existing approaches in decoding the network topology, the issue remains of whether quantitative information about node-to-node coupling, namely, the detailed dynamical coupling terms among various nodes in the network, can be inferred purely from measured time series.

In this paper, we articulate a framework that enables a full reconstruction of coupled oscillator networks whose vector fields consist of a limited number of terms in some suitable base of expansion. Our basic idea is that the mathematical functions determining the dynamical couplings in a physical network can be expressed by power series expansions. The task is then to estimate all the nonzero coefficients. Since the underlying coupling functions are unknown, the power series can contain high-order terms. The number of coefficients to be estimated can therefore be quite large. According to conventional wisdom this would be a difficult problem as a large amount of data is required and the computations involved

(a) E-mail: wenxuw@gmail.com

can be extremely demanding. However, the number of nonzero coefficients may be only a few so that the vector of coefficients is effectively sparse. As such, the recently developed idea of compressive sensing provides a viable solution to the problem, whose key feature is to reconstruct a sparse signal from a limited number of observations [14–17]. Since the requirements for the observations can be considerably relaxed as compared with those associated with conventional signal reconstruction schemes, compressive sensing has received much recent attention and it is becoming a powerful technique to obtain high-fidelity signal for applications where sufficient observations are not available. We shall articulate a general methodology to cast the problem of network reconstruction into the framework of compressive sensing, show that the power series coefficients associated with the interactions among nodes can be accurately estimated, and demonstrate the power of our method by using a variety of model and real-world networks.

Generally, the problem of compressive sensing can be described as to reconstruct a sparse vector $\mathbf{a} \in R^N$ from linear measurements $\mathbf{X}$ about $\mathbf{a}$ in the form: $\mathbf{X} = \mathbf{G} \cdot \mathbf{a}$, where $\mathbf{X} \in R^M$ and $\mathbf{G}$ is an $M \times N$ matrix. By definition, the number of measurements is much less than the number of components of the unknown signal, *i.e.*, $M \ll N$. Accurate reconstruction can be achieved by solving the following convex optimization problem [18]:

$$\min \|\mathbf{a}\|_1 \quad \text{subject to} \quad \mathbf{G} \cdot \mathbf{a} = \mathbf{X}, \tag{1}$$

where $\|\mathbf{a}\|_1 = \sum_{i=1}^{N} |\mathbf{a}_i|$ is the L_1 norm of vector $\mathbf{a}$. Solutions of the convex optimization problem (1) have been worked out recently [18,19].

We first show that the inverse problems of predicting network topology can be cast in the form (1). A complex networked system can be viewed as a large dynamical system that generates oscillatory time series at various nodes. In general, the dynamics at a node can be written as

$$\dot{\mathbf{x}}_i = \mathbf{F}_i(\mathbf{x}_i) + \sum_{j=1, j\neq i}^{N} \mathbf{C}_{ij}(\mathbf{x}_j - \mathbf{x}_i) \quad (i = 1, \ldots, N), \tag{2}$$

where $\mathbf{x}_i \in R^m$ represents the set of externally accessible dynamical variables of node i, N is the number of accessible nodes, and $\mathbf{C}_{ij}$ is the coupling matrix between the dynamical variables at nodes i and j denoted by

$$\mathbf{C}_{ij} = \begin{pmatrix} c_{ij}^{1,1} & c_{ij}^{1,2} & \cdots & c_{ij}^{1,m} \\ c_{ij}^{2,1} & c_{ij}^{2,2} & \cdots & c_{ij}^{2,m} \\ \cdots & \cdots & \cdots & \cdots \\ c_{ij}^{m,1} & c_{ij}^{m,2} & \cdots & c_{ij}^{m,m} \end{pmatrix}. \tag{3}$$

In $\mathbf{C}_{ij}$, the superscripts kl $(k, l = 1, 2, \ldots, m)$ stand for the coupling from the k-th component of the dynamical variable at node i to the l-th component of the dynamical variable at node j. For any two nodes, the number of possible coupling terms is m^2. If there is at least one nonzero element in the matrix $\mathbf{C}_{ij}$, nodes i and j are coupled and, as a result, there is a link (or an edge) between them in the network. Generally, more than one element in $\mathbf{C}_{ij}$ can be nonzero. Likewise, if all the elements of $\mathbf{C}_{ij}$ are zero, there is no coupling between nodes i and j. The connecting topology and the interaction strengths among various nodes of the network can be predicted if we can estimate the coupling matrix $\mathbf{C}_{ij}$ from time series measurements.

Generally, our method consists of the following two steps. First we rewrite eq. (2) as

$$\dot{\mathbf{x}}_i = \left[\mathbf{F}_i(\mathbf{x}_i) - \sum_{j=1, j\neq i}^{N} \mathbf{C}_{ij}\mathbf{x}_i \right] + \sum_{j=1, j\neq i}^{N} \mathbf{C}_{ij}\mathbf{x}_j, \tag{4}$$

where the first term on the right-hand side is exclusively a function of $\mathbf{x}_i$, while the second term is a function of variables of other nodes (couplings). We define the first term to be $\mathbf{\Gamma}_i(\mathbf{x}_i)$, which is unknown. In general, the k-th component of $\mathbf{\Gamma}_i(\mathbf{x}_i)$ can be represented by a power series of order up to n:

$$\begin{aligned} [\mathbf{\Gamma}_i(\mathbf{x}_i)]_k &\equiv \left[\mathbf{F}_i(\mathbf{x}_i) - \sum_{j=1, j\neq i}^{N} \mathbf{C}_{ij}\mathbf{x}_i \right]_k \\ &= \sum_{l_1=0}^{n} \sum_{l_2=0}^{n} \cdots \sum_{l_m=0}^{n} [(\alpha_i)_k]_{l_1,\ldots,l_m} \\ &\quad [(\mathbf{x}_i)_1]^{l_1} [(\mathbf{x}_i)_2]^{l_2} \cdots [(\mathbf{x}_i)_m]^{l_m}, \end{aligned} \tag{5}$$

where $(\mathbf{x}_i)_k$ $(k = 1, \ldots, m)$ is the k-th component of the dynamical variable at node i, the total number of products is $(1+n)^m$, and $[(\alpha_i)_k]_{l_1,\ldots,l_m} \in R^m$ is the coefficient scalar of each product term, which is to be determined from measurements as well. Note that terms in eq. (5) are all possible products of different components with different power of exponents. As an example, for $m = 2$ (the components are x and y) and $n = 2$, the power series expansion is $\alpha_{0,0} + \alpha_{1,0}x + \alpha_{0,1}y + \alpha_{2,0}x^2 + \alpha_{0,2}y^2 + \alpha_{1,1}xy + \alpha_{2,1}x^2y + \alpha_{1,2}xy^2 + \alpha_{2,2}x^2y^2$.

Second, we rewrite eq. (4) as

$$\dot{\mathbf{x}}_i = \mathbf{\Gamma}_i(\mathbf{x}_i) + \mathbf{C}_{i1}\mathbf{x}_1 + \mathbf{C}_{i2}\mathbf{x}_2 + \cdots + \mathbf{C}_{iN}\mathbf{x}_N. \tag{6}$$

Our goal is to estimate the various coupling matrices $\mathbf{C}_{ij}(j = 1, \ldots, i-1, i+1, \ldots, N)$ and the coefficients of $\mathbf{\Gamma}_i(\mathbf{x}_i)$ from sparse time series measurements. According to the compressive-sensing theory, to reconstruct the coefficients of eq. (6) from a small number of measurements, most coefficients should be zero, *i.e.*, the sparse signal requirement. To include as many coupling forms as possible, we expand each term $\mathbf{C}_{ij}\mathbf{x}_j$ in eq. (6) as a power series in the same form of $\Gamma_i(\mathbf{x}_i)$ but with different coefficients:

$$\dot{\mathbf{x}}_i = \mathbf{\Gamma}_1(\mathbf{x}_1) + \mathbf{\Gamma}_2(\mathbf{x}_2) + \cdots + \mathbf{\Gamma}_N(\mathbf{x}_N). \tag{7}$$

This setting not only includes many possible coupling forms but also ensures that the sparsity condition is satisfied so that the prediction problem can be formulated in the compressive-sensing framework. For an arbitrary node i, information about node-to-node coupling, or about the network connectivity, is contained completely in $\mathbf{\Gamma}_j (j \neq i)$. For example, if in the equation of i, a term in $\mathbf{\Gamma}_j (j \neq i)$ is not zero, there then exists coupling between i and j with the strength given by the coefficient of the term. Subtracting the coupling terms $-\sum_{j=1, j\neq i}^{N} \mathbf{C}_{ij}\mathbf{x}_i$ from $\mathbf{\Gamma}_i$ in eq. (5), which is the sum of coupling coefficients of all $\mathbf{\Gamma}_j (j \neq i)$, the node dynamics $\mathbf{F}_i(\mathbf{x}_i)$ can be obtained. Therefore, once the coefficients of eq. (7) have been determined, the node dynamics and couplings among nodes are all known.

To explain our method in a more detailed and concrete manner, we focus on one component of the dynamical variable at all nodes in the network, say component 1. (Procedures for other components are similar.) For each node, we first expand the corresponding component of the vector field into a power series up to power n. For a given node, due to the interaction between this component and other $(m-1)$ components of the vector field, there are $(n+1)^m$ terms in the power series. The number of coefficients to be determined for each individual node dynamics is thus $(n+1)^m$. Now consider a specific node, say node i. For every other node in the network, possible couplings from node i indicates the need to estimate another set of $(n+1)^m$ power series coefficients in the functions of $\mathbf{\Gamma}_j(\mathbf{x}_j)$. There are in total $N(n+1)^m$ coefficients that need to be determined. The vector $\mathbf{a}$ to be determined in the compressive-sensing framework contains then $N(n+1)^m$ components. For example, to construct the measurement vector $\mathbf{X}$ and the matrix $\mathbf{G}$ for the case of $m=3$ (dynamical variables x, y, and z) and $n=3$, we have the following explicit dynamical equation for the first component of the dynamical variable of node i:

$$\begin{aligned}\Gamma_i(x_i) \;=\; & (a_i)_{000}\cdot x_i^0 y_i^0 z_i^0 + \cdots + (a_i)_{003}\cdot x_i^0 y_i^0 z_i^3 \\ & + (a_i)_{010}\cdot x_i^0 y_i^1 z_i^0 + \cdots + (a_i)_{100}\cdot x_i^1 y_i^0 z_i^0 \\ & + \cdots + (a_i)_{333}\cdot x_i^3 y_i^3 z_i^3. \end{aligned} \tag{8}$$

We can denote the coefficients of $\Gamma_i(x_i)$ by $\mathbf{a}_i = [(a_i)_{000}, (a_i)_{001}, \ldots, (a_i)_{333}]^T$. Assuming that measurements $\mathbf{x}_i(t)$ $(i=1,\ldots,N)$ at a set of time $t_1, t_2, \ldots, t_M$ are available, we denote

$$\begin{aligned}\mathbf{g}_i(t) = \big[& x_i(t)^0 y_i(t)^0 z_i(t)^0, x_i(t)^0 y_i(t)^0 z_i(t)^1, \ldots, \\ & x_i(t)^3 y_i(t)^3 z_i(t)^3\big], \end{aligned} \tag{9}$$

such that $\Gamma_i[x_i(t)] = \mathbf{g}_i(t)\cdot\mathbf{a}_i$. According to eq. (8), the measurement vector can be chosen as $\mathbf{X} = [\dot{x}_i(t_1), \dot{x}_i(t_2), \ldots, \dot{x}_i(t_M)]^T$, which can be calculated from time series. Finally, we obtain the following equation in the form $\mathbf{X} = \mathbf{G}\cdot\mathbf{a}$:

$$\begin{pmatrix} \dot{x}_i(t_1) \\ \dot{x}_i(t_2) \\ \vdots \\ \dot{x}_i(t_M) \end{pmatrix} = \begin{pmatrix} \mathbf{g}_1(t_1) & \mathbf{g}_2(t_1) & \cdots & \mathbf{g}_N(t_1) \\ \mathbf{g}_1(t_2) & \mathbf{g}_2(t_2) & \cdots & \mathbf{g}_N(t_2) \\ \vdots & \vdots & \vdots & \vdots \\ \mathbf{g}_1(t_M) & \mathbf{g}_2(t_M) & \cdots & \mathbf{g}_N(t_M) \end{pmatrix} \times \begin{pmatrix} \mathbf{a}_1 \\ \mathbf{a}_2 \\ \vdots \\ \mathbf{a}_N \end{pmatrix}, \tag{10}$$

where, to ensure the restricted isometry property [18], we normalize it by dividing elements in each column by the L_2 norms of that column: $(\mathbf{G})_{ij} = (\mathbf{G})_{ij}/L_2(j)$ with $L_2(j) = \sqrt{\sum_{i=1}^{M}[(\mathbf{G})_{ij}]^2}$. After $\mathbf{a}$ is determined via some standard compressive-sensing algorithm, the coefficients are given by $\mathbf{a}/L_2$. To determine the set of power series coefficients corresponding to a different component of the dynamical variable, say component 2, we simply replace the measurement vector by $\mathbf{X} = [\dot{y}_i(t_1), \dot{y}_i(t_2), \ldots, \dot{y}_i(t_M)]^T$ and use the same matrix $\mathbf{G}$. This way all coefficients can be estimated. After the equations of all components of i are determined, we can repeat this process for all other nodes. Finally, the system can be reconstructed.

To illustrate our method, we consider networks of coupled chaotic Lorenz and Rössler oscillators. The classical Lorenz and Rössler systems are given by $[\dot{x}, \dot{y}, \dot{z}] = 10(y-x), x(28-z)-y, xy-(8/3)z]$ and $[\dot{x}, \dot{y}, \dot{z}] = -y-z, x+0.2y, 0.2+z(x-5.7)]$, respectively. Since $m=3$, we choose the power series of x, y and z such that $l_1+l_2+l_3 \leqslant 3$. The total number of the coefficients to be estimated is then $N\sum_{i=1}^{3}(i+1)(i+2)/2+1 = 19N+1$, where $i = l_1+l_2+l_3$ ranges from 1 to 3, N denotes the total number of nodes and 1 is due to the constant term. To demonstrate the applicability of our method to complex networks of different topology, we consider random and scale-free networks. In particular, the Lorenz oscillator network is chosen to be a Erdős-Rényi type of homogeneous random network [20], generated by assuming a small probability of link for any pair of nodes. The coupling between node dynamics is assumed to occur between the y and the z variables in the Lorenz equations, leading to the following coupling matrix: $c_{ij}^{3,2} = 1$ if nodes i and j are connected and $c_{ij}^{3,2} = 0$, otherwise. The Rössler oscillator network is assumed to be a Barabási-Albert type of scale-free network [21] with a heterogeneous degree distribution. The coupling scheme is $c_{ij}^{1,3} = 1$ for link between i and j. Both types of network structures are illustrated schematically in fig. 1. To generate time series, we integrate the whole networked system by using time step $h = 10^{-4}$ for 6×10^6 steps. However, the number of "measured" data points required for our method to be successful can be orders of magnitude less than 6×10^6, *a fundamental advantage of compressive-sensing method*. Specifically, we randomly collect measurements from the integrated time series and

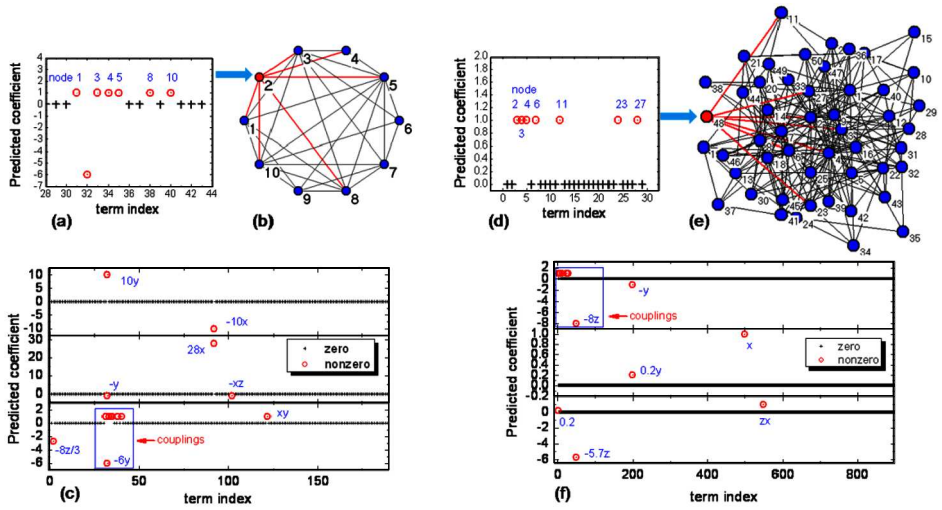

Fig. 1: (Colour on-line) (a) Predicted coupling terms in the z variable for node #2 in the random network (b) of 10 coupled chaotic Lorenz oscillators. (c) Predicted terms in the dynamics of node #2 and couplings between node #2 and other nodes. (d) Predicted coupling terms in the x-variable for node #48 in the scale-free network (e) of 50 coupled chaotic Rössler oscillators. (f) Predicted terms in the dynamics of node #48 and couplings between node #48 and other nodes. In (c) and (f), top to bottom panels: predicted terms with coefficients in the x, y and z variables, where the corresponding true values of the existent terms are marked. In (a) and (d), the node numbers corresponding to the existing terms are marked and the coupling forms are $c^{3,2}$ and $c^{1,3}$, respectively. Here, the term index refers to the order of to be predicted coefficients appearing in eq. (7) and in the vector $\mathbf{a}$ of eq. (10). The average degrees $\langle k \rangle$ for the random and scale-free networks are 6 and 10, respectively. The number of data points used for prediction is 140 and the time interval for data collection is $\Delta t = 1$.

the number of elements in each row of the matrix $\mathbf{G}$ is given by $N(n+1)^m$.

Figure 1 shows some representative results. For the random Lorenz network, we show the inferred coefficients of node #2 associated with both the couplings with other nodes (fig. 1(a)) and those with its own dynamics (fig. 1(a)). The term index is arranged from low to high values, corresponding to the order from low to high node number. The predicted coupling strengths between node #2 and others are shown in fig. 1(a), where each term according to its index corresponds to a specific node. Nonzero terms belonging to nodes other than node #2 indicate inter-node couplings. The predicted interactions with nonzero coefficients (the value is essentially unity) are in agreement with the neighbors of node #2 in the sample random network in fig. 1(b). The term 32 related to $-6y$ is the coupling strength from node #2, which equals the sum of the coupling strengths from the other connected nodes. Figure 1(c) displays the inferred coefficients for both node dynamics and coupling terms in the three components x, y and z. All predicted terms with nonzero coefficients are in agreement with those in the equations of the dynamics of node #2, together with the inter-node coupling terms $c^{3,2}$.

Figure 1(d) shows the predicted links between node #48 and others in a Rössler oscillator network with a scale-free structure. All existing couplings have been accurately inferred, as compared to the structure presented in fig. 1(e), even though the interaction patterns among nodes are heterogeneous. Both the detected local dynamical and coupling terms associated with node #48 are indicated in fig. 1(f), where in the x-component, the term $-8z$ is the combination of the local-dynamical term $-z$ and the coupling of node #48 with 7 neighboring nodes. Since all the couplings have been successfully detected, the local-dynamical term $-z$ in the x-component can be separated from the combination, so that all terms of node #48 are predicted. We have also examined all nodes in the two network systems and find that the method is effective for all oscillators, enabling a complete and accurate reconstruction of the underlying complex networked system.

To quantify the performance of our method with respect to the amount of required data as well as different network properties, we investigate the prediction errors which are defined separately for nonzero (existing) and zero terms in the dynamical equations. The relative error of a nonzero term is defined as the ratio to the true value of the absolute difference between the predicted and the true value. The average over the errors of all terms in a component is the prediction error E_{nz} of nonzero terms for the component. In contrast, a relative error for a zero (nonexistent) term cannot be defined, so it is necessary to use the absolute error. Figure 2(a) shows the errors E_{nz} and E_z as functions of the number of data points collected with fixed sampling frequency for the random network of Lorenz oscillators and the scale-free network of Rössler oscillators. We see that if the number of data points in the time series used for prediction is not large

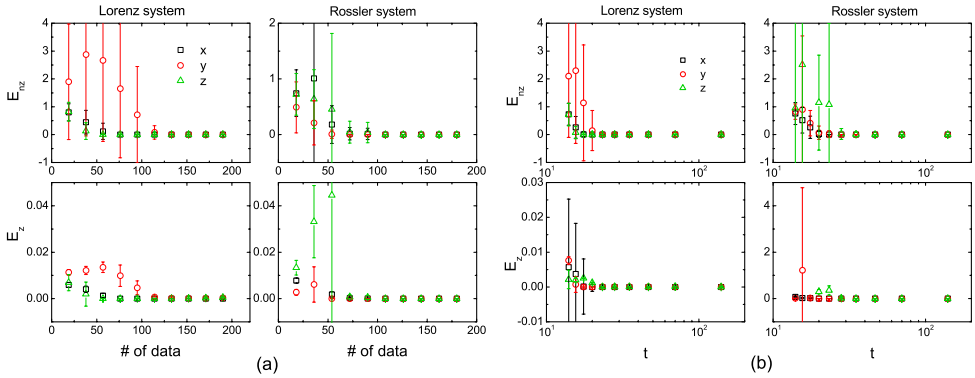

Fig. 2: (Colour on-line) Prediction errors E_{nz} and E_z as functions of (a) the number of data points and (b) length t of time series for the random network of Lorenz oscillators and the scale-free network of Rössler oscillators. In (a) the time interval for collecting a data point in the time series is $\Delta t = 1$. In (b), the number of data points used is fixed to be 140 for different t. All results are obtained by the average over 10 independent realizations and the error bars represent standard deviations.

enough, E_{nz} and E_z can be quite large. However, when the number of data points exceeds some critical value, *e.g.*, 140 for the Lorenz network and 100 for the Rössler network, the prediction errors become practically zero. In all cases, the number of required data points is much smaller than the number of terms in the power series function, a main advantage of the compressive-sensing technique. Insofar as the number of data points exceeds a critical value, the prediction errors are effectively zero, indicating the robustness of the reconstructions. Figure 2(b) shows the errors with respect to different length t of the time series for a fixed number of collected data, where the sampling frequency is inversely proportional to t. We see that when t is relatively large, *e.g.*, $t > 20$ for the Lorenz network and $t > 30$ for the Rössler network, E_{nz} and E_z are small and the reconstructions are accurate. Note that, if the sampling frequency is high, the number of data points is not able to cover the dynamics in the whole phase space. In order to obtain a faithful prediction of the whole system, the sampling frequency must be sufficiently low.

Another important question is how the structural properties of the network affect the prediction precision. To address this question, we calculate the dependence of the prediction error on the average degree $\langle k \rangle$ and the network size N. We find that, regardless of the network size, insofar as the network connections are sparse, the prediction errors remain to be quite small, providing further support for the robustness of our compressive-sensing–based method.

Our computations have demonstrated that, despite the small prediction errors, all existing links in the original network can be predicted extremely reliably. To further quantify the performance of our method for predicting network structures, we compute the success rates for existing links (SREL) and nonexisting links (SRNL), defined to be the ratio between the number of successfully predicted links and total number of links and the ratio of the number of correctly predicted nonexisting links to the total number of nonexisting links, respectively. Figure 3 shows the success rates as functions of the number of data points and t for both random Lorenz and Rössler oscillator networks. We observe that, when the number of data points and t are sufficiently large, both SREL and SRNL reach 100%. The inset in the upper-right panel shows the distribution of coupling strengths in the Rössler network. For all tested numbers of data points (> 54), there exist two sharp peaks centered at $c = 0$ and $c = 1$, corresponding to the absence of coupling and the existing coupling of strength 1.0, respectively. The narrowness of the two peaks in the distribution makes it feasible to distinguish existing links (with nonzero coupling strength) from nonexistent links (effectively with zero coupling). This provides an explanation for the 100% success rates shown in fig. 3.

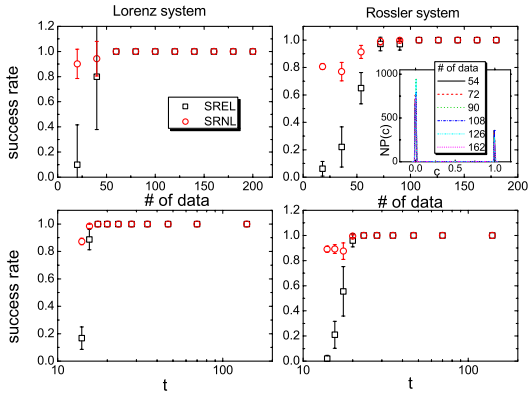

Fig. 3: (Colour on-line) Success rates of existing links SREL and nonexisting links SRNL as functions of the number of data points and length t of time series for random Lorenz and Rössler networks. The inset in the upper-right panel shows the distribution of coupling strength in the Rössler network for different numbers of data points.

Finally, we test our method on a number of real-world networks, ranging from social to biological and technological networks. Again we assume the node dynamics to be of the Lorenz and Rössler types. For five real-world networks,

Table 1: Prediction errors E_{nz} and E_z for five real-world networks: (1) dolphin social network [22], (2) friendship network of karate club [23], (3) network of political book purchases [24], (4) electric circuit networks [25], and (5) the neural network of *C. Elegans* [26].

	Lorenz		Rössler	
	E_{nz}	E_z	E_{nz}	E_z
1	3.6×10^{-3}	7.4×10^{-6}	2.8×10^{-3}	2.2×10^{-7}
2	3.3×10^{-3}	3.6×10^{-6}	1.9×10^{-3}	2.7×10^{-7}
3	3.8×10^{-3}	8.3×10^{-5}	2.8×10^{-3}	2.1×10^{-7}
4	4.4×10^{-3}	5.8×10^{-6}	2.9×10^{-3}	2.7×10^{-7}
5	1.1×10^{-3}	1.9×10^{-5}	2.8×10^{-3}	2.2×10^{-7}

the prediction errors are shown in table 1. We observe that all errors are small, indicating the potential applicability of our method to real-world networks.

Some remarks concerning the general applicability of our method and computational requirement are in order. 1) While we have used linear coupling schemes in our numerical test, the compressive-sensing–based prediction method is expected to be applicable even for nonlinear coupling, as any such coupling function can be approximated by a power series expansion. We have also examined networks of nonidentical oscillators, for example networks whose nodes are a mixture of Lorenz and Rössler oscillators, and found that the networked system can be accurately reconstructed. 2) In general, the number of required data for successful reconstruction depends on the sparsity of the coefficient vector **a**. If **a** is sparser, less data is needed. 3) Based on our experience, if the prediction base is sufficiently wide to include all terms in the system equation as a small subset, high-accuracy prediction can be guaranteed, regardless of the mathematical forms of the terms in the equations. 4) Our method is robust for weak noise due to the optimization nature of the compressive-sensing paradigm. However, for larger noise, because of the need to estimate various derivatives to some reasonable precision, the method may fail. This is not a deficiency of the compressive-sensing paradigm. Insofar as derivatives can be estimated reliably, the compressive-sensing–based method can always yield optimal and accurate solutions.

In summary, we have articulated a method based on compressive sensing for predicting and reconstructing complex dynamical networks from measured time series. Extensive computations have revealed that both nonlinear node dynamics and node-to-node interactions can be accurately predicted, leading to reliable and robust reconstruction of the underlying networked system, as characterized by near-zero prediction errors regardless of the nature of the node dynamics and the network structure. Although all the examples of node dynamics used in the paper are polynomial vector fields, we have examined other expansion bases such as trigonometric functions. If the prediction base is sufficiently wide to include all terms in the system equations as a small subset, high-accuracy prediction can be guaranteed, regardless of the mathematical forms of the terms in the equations. These features make our method appealing to predicting general complex networked systems with extremely low data requirement.

* * *

We thank Dr Q.-F. Chen for discussions. This work was supported by AFOSR under Grants No. FA9550-10-1-0083 and No. FA9550-09-1-0260, and by NSF under Grants No. CDI-1026710 and No. BECS-1023101.

REFERENCES

[1] Newman M. E. J., *SIAM Rev.*, **45** (2003) 167.
[2] Timme M., *Phys. Rev. Lett.*, **98** (2007) 224101.
[3] Napoletani D. and Sauer T. D., *Phys. Rev. E*, **77** (2008) 026103.
[4] Wang W.-X., Chen Q., Huang L., Lai Y.-C. and Harrison M. A. F., *Phys. Rev. E*, **80** (2009) 016116.
[5] Ren J., Wang W.-X., Li B. and Lai Y.-C., *Phys. Rev. Lett.*, **104** (2010) 058701.
[6] Gardner T. S., di Bernardo D., Lorenz D. and Collins J. J., *Science*, **301** (2003) 102.
[7] Bansal M., Belcastro V., Ambesi-Impiombato A. and di Bernardo D., *Mol. Syst. Biol.*, **3** (2007) 78.
[8] Geier F., Timmer J. and Fleck C., *BMC Syst. Biol.*, **1** (2007) 11.
[9] Hecker M., Lambeck S., Toepferb S., van Someren E. and Guthke R., *BioSystems*, **96** (2009) 86.
[10] Grün S., Diesmann M. and Aertsen A., *Neural Comput.*, **14** (2002) 43.
[11] Gütig R., Aertsen A. and Rotter S., *Neural Comput.*, **14** (2002) 121.
[12] Pipa G. and Grün S., *Neurocomputing*, **52** (2003) 31.
[13] Clauset A., Moore C. and Newman M. E. J., *Nature*, **453** (2008) 98.
[14] Candès E., *Proceedings of the International Congress of Mathematicians (Madrid, Spain) 2006.*
[15] Baraniuk R., *IEEE Signal Process. Mag.*, **24** (2007) 118.
[16] Candès E. and Wakin M., *IEEE Signal Process. Mag.*, **25** (2008) 21.
[17] Romberg J., *IEEE Signal Process. Mag.*, **25** (2008) 14.
[18] Candès E., Romberg J. and Tao T., *IEEE Trans. Inf. Theory*, **52** (2006) 489; *Commun. Pure Appl. Math.*, **59** (2006) 1207.
[19] Candès E. and Romberg J., `http://www.acm.caltech.edu/l1magic`.
[20] Erdős P. and Rényi, *Publ. Math. Debrecen*, **6** (1959) 290.
[21] Barabási A.-L. and Albert R., *Science*, **286** (1999) 509.
[22] Lusseau D., Schneider K., Boisseau O. J., Haase P., Slooten E. and Dawson S. M., *Behav. Ecol. Sociobiol.*, **54** (2003) 96.
[23] Zachary W. W., *J. Anthropol. Res.*, **33** (1977) 452.
[24] `http://www.orgnet.com/cases.html`.
[25] Milo R., Itzkovitz S., Kashtan N., Levitt R., Shen-Orr S., Ayzenshtat I., Sheffer M. and Alon U., *Science*, **303** (2004) 1538.
[26] Watts D. J. and Strogatz, *Nature*, **393** (1998) 440.